Comparison of computed vs. measured lateral load/deflection response of ACIP piles

K.E. Tand, P.E., Principal Engineer, Kenneth E. Tand & Associates
C. Vipulanandan, Ph.D., P.E., Chairman of the U of H Civil Engineering Dept.

Introduction

Five auger cast-in-place piles (ACIP) were installed at the National Geotechnical Experimentation Site located at the University of Houston campus in Houston, Texas in December 1996. Lateral load tests were performed on four of the piles in January 1997. The purpose of these tests was to evaluate the feasibility for design and construction of ACIP piles to support concrete screen walls subjected to large wind forces along highways in urban areas.

Subsoil Profile

The site is located on a Pleistocene age deltaic deposit known locally as the Beaumont formation. The Beaumont formation is about 8 meters deep at the test site, and it is underlain by an older geologic formation known as the Montgomery formation. The subsoils in both formations are primarily clay with occasional interbedded seams and layers of sand and silt. The consistency of the clays is generally stiff to very stiff, and they have been overconsolidated due to desiccation.

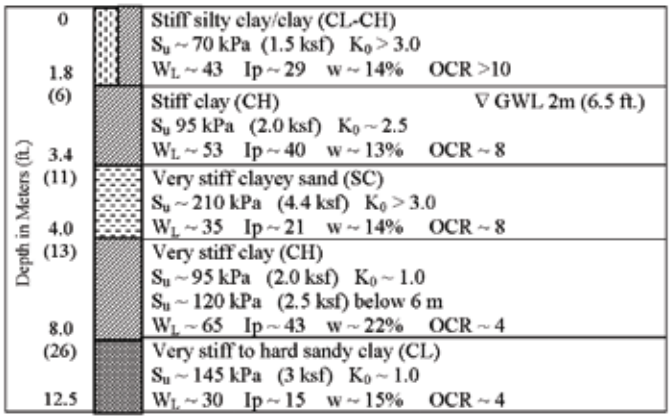

Fig 1: Generalized Subsoil Profile

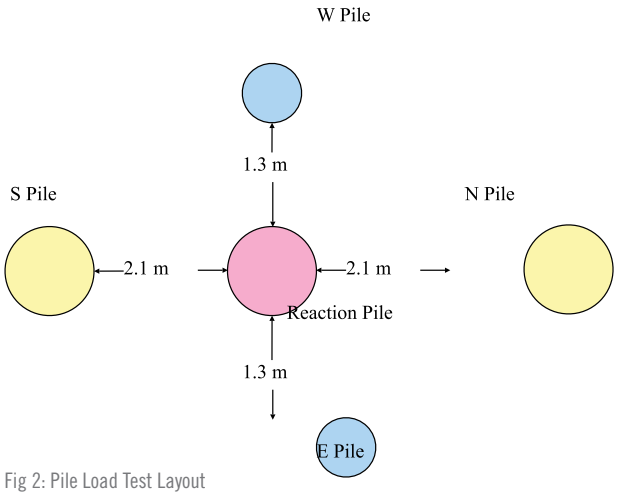

Fig 2: Pile Load Test Layout

Photo 1: Load Testing a 0.91 m Diameter ACIP Pile

The first major silt/sand stratum occurs at a depth of 14 m (47 ft) which is below the depth of influence of the test piles. The water level was at a depth of about 2 m (6.5 ft) below grade at the time of the load tests.

After deposition, vertical fissures were formed due to shrinkage caused by drying, and the cracks at the surface were probably more than 5 cm (2 in) wide visually estimated from presently occurring wet/dry cycles. Soil from the surface was washed down into these cracks during periods of heavy rain. The soft sediments in the cracks were then compressed when the clays swelled leaving locked-in horizontal stress. This process was repeated throughout Pleistocene to Modern geologic times, and K_0 values of 3.0 and greater have been measured in the upper 4 m (13 ft) at this site. The process of desiccation and subsequent rewetting caused cyclic shearing displacements in the clay mass that produced polished failure planes referred to as slickensides. The slickensides are widely variable in size and orientation. The clays are spatially inhomogeneous, and exhibit some anisotropic properties due to their stress history.

The joints and horizontal locked-in stress affect the strength, deformation, and permeability properties of the clays. The soil parameters have been extensively studied at this site and they are summarized in Fig. 1. A more detailed summary of the database can be found on the web site at www.unh.edu/nges. The laboratory and in situ tests in the database indicate a wide range in the strength/deformation properties of the clays due to the effects of secondary structure, loading stress path, and possible sample disturbance.

Test Piles and Instrumentation

The pile load test arrangement is shown on Fig. 2. The N pile was 0.91 m (36 in) in diameter and 10.7 m (35 ft) long, and the W pile was 0.46 m (18 in) in diameter and 10.7 m (35 ft) long. The S pile was 0.91 m (36 in) in diameter and 6.1 m (20 ft) long, and the E pile was 0.46 m (18 in) in diameter and 6.1 m (20 ft) long.

The piles were installed using a continuous hollow stem flight auger rotated into the ground at a rate of 400 to 1,200 mm/min (16 to 47 in/min). Immediately after reaching the design depth, the augers were slowly withdrawn while pumping high strength grout into the pile. Grouting was monitored using a pile integrity recorder, and the ratio of the pumped versus theoretical grout volume ranged from 1 to more than 2 (average of 1.3). The soil was stiff to very stiff clay, and most (if not all) of the grout in excess of the pile volume was lost at the surface when removing the spoils.

The grout mix was comprised of Portland cement, fly ash, sand, water and a fluidizer. The compressive strength of the field mix was 38 MPa (5,500 psi), and the tensile strength was 2.0 MPa (280 psi) at 28 days.

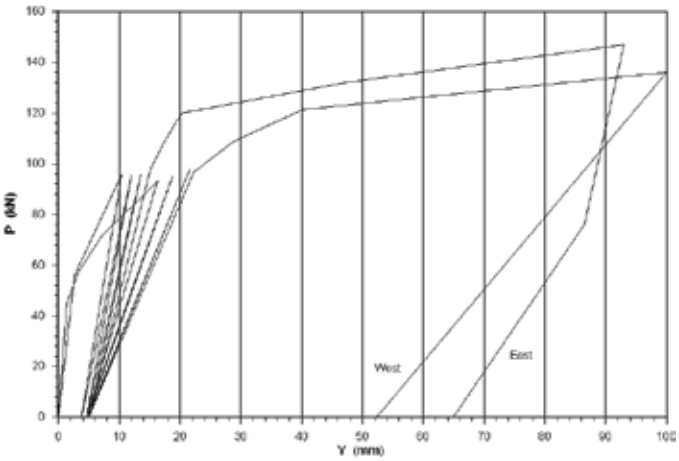

Fig 3: Lateral load-deflection curves for E & W Piles

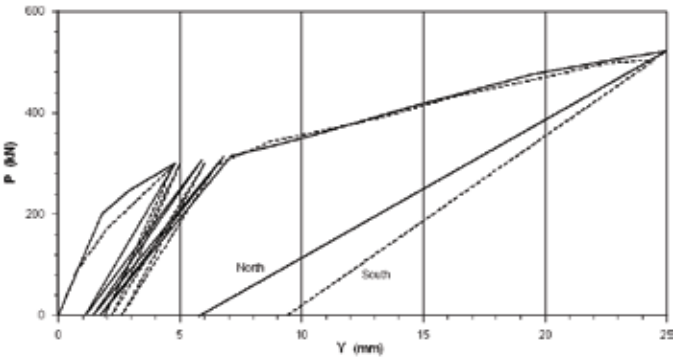

Fig 4: Lateral load-deflection curves for S & N Piles

Immediately after cleaning the top of the pile heads with a screen, a full length rebar cage was inserted into the piles. The rebar cages for the 0.46 m diameter piles were comprised of six number 6 vertical rebars with number 3 ties spaced at 15 cm (6 in) centers. The cages for the 0.91 m diameter piles were comprised of eight number 10 vertical rebars with number 4 ties spaced at 23 cm (9 in) centers.

As shown on Photo 1, two ABS tubes were installed in each pile. They were used for sonic logging to check the integrity of the piles prior to the load tests. Based on results of the sonic tests, the piles were found to be free of defects such as voids or cracks.

One of the ABS tubes in each pile was later used as a guide to run an inclinometer instrument down the piles during the lateral load tests to measure the rotation during loading.

Pile Load Tests

The piles were load tested 28 days after installation. The lateral load was applied at about 15 cm (6 in) above the ground level so that only a very small bending moment was induced into the pile head during loading.

The load was applied using a hydraulic jack, and it was measured using an electronic load cell. As shown on Photo 1, the jack and load cells were housed inside a steel pipe strut. Lateral deflections at the pile head were measured using an electronic measuring gauge mounted on the back side of the piles with the tip set to a wooden reference beam. The below grade deformations were measured using an electronic inclinometer.

The E & W piles (0.46 m diameter) were loaded in 4 increments to about 55 kN (12 kips), and each load was held for a period of 15 minutes. The piles were then unloaded back to “0”, and the load was cycled 4 times to simulate wind loading. After cycling, they were loaded in increments to about 95 kN (21 kips), and then again cycled 4 times. The piles were finally loaded in increments until the deflections exceeded 90 mm (3.5 in).

The N & S piles (0.91 m diameter) were loaded in 4 increments to about 172 kN (39 kips), and each load was held for a period of 15 minutes. The piles were cycled as described above, and then they were loaded to about 300 kN (68 kips) and cycled 4 times again. The piles were finally loaded in increments to a deflection of 25 mm (1 in).

The load/deflection relationships are shown graphically in Figs. 3 & 4. During the initial cycling, the deflections were so small that they are not shown on the graphs for clarity. Note that non-linear pile deflections started to occur at about 60 kN (14 kips) for the E & W piles, and at about 200 kN (45 kips) for the N & S piles.

The initial load/deflection response of the N pile was slightly stiffer than the shorter S pile. However, the initial load/deflection response of the W pile was softer than the E pile even though it had 4.6 m (15 ft) more embedment. The authors speculate that subsoil variations were present even though these piles were only 4 m (13 ft) apart. Perhaps, the slickensides and fissures in the clay were orientated in an unfavorable pattern in front of the W pile. However, there could have been an undetected defect in this pile.

The inclinometer readings indicated that a plastic hinge formed at a depth of about 2.1 m (7 ft) in both the E & W piles, even though the W pile had 4.6 m (15 ft) more embedment. The plastic hinge formed at a depth of about 4.5 m (15 ft) in the larger diameter S pile. The inclinometer tube in the N pile was plugged during grouting, and thus data was not available for this pile. However, the load/deflection response was so similar for the N&S piles that it is assumed that the hinge occurred at the same depth.

Comparison of computed vs. measured lateral load/deflection response of ACIP piles

Continuation

FE Analysis

The numerical model employed in the FE analysis for the S pile (typical for all piles) is shown in Fig. 5. The calculations were performed using PLAXIS 3D Foundations V.2 with about 2,000 elements. The small strain hardening soil model was used to model the stiff to very stiff clay.

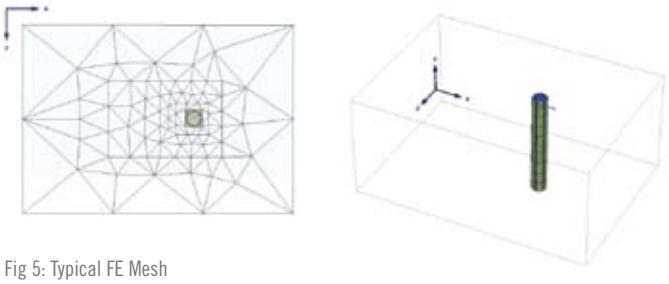

Fig 5: Typical FE Mesh

The authors speculate that the stiffness of the piles affected the load/deflection response as much as the strength and stiffness of the clay subsoils. To study its' influence, the piles were modeled as circular piles with a steel shell. A wall element with the equivalent EI of the rebar was input to model the stiffness of the rebar.

A mass concrete pile is most often modeled using linear elastic properties of the pile materials. However, the stiffness will be overestimated if tensile strains are large enough to crack the concrete. The cracks reduce the moment of inertia, and this is a continuing process as increasing deflections cause the cracks to propagate. The moment of inertia must be adjusted to reflect the correct state of stress in the pile whether conventional methods of analysis such as Brom's procedure or numerical methods such as finite element or beam-on-elastic foundation procedures are used. One objective of this study is to evaluate whether the pile materials can be modeled so that the moment of inertia is numerically adjusted during the FE calculations.

The laboratory compression tests that had been performed on the grout cylinders were modeled using PLAXIS 2D Version 8, and the following parameters for the Mohr-Columb model were back calculated in our analysis by best fitting the stress-strain data:

Youngs' Modulus	Cohesion	ϕ	Tension
2.5 x 10^7 MPa	7.2 MPa	40°	1.9 MPa
(5.2 x 10^5 ksf)	(150 ksf)	-	(40 ksf)

The following basic procedures were used during the FE analysis:

- The initial K_0 conditions were generated using a 0.3 m (1 ft) thick "dummy soil layer" with a unit weight of 943 kN/m^3 (6,000 pcf) in the initial phase. Thus, the gravity loading induced a preconsolidation pressure of 216 kP_a (6,000 psf). This layer was then turned off for the subsequent calculations. The FE computed K_0 was 2.9 at 1.2 m (4 ft), and 2.6 at 3.6 m (12 ft). These values correlate reasonably well with those reported in the U of H database.
- Effective stress parameters for the stiff to very stiff clays were used as input, but the analysis was performed using the undrained mode to simulate the rapid rate of loading.
- Initially, soil parameters were selected from Tand and O'Neill's article published in the PLAXIS Bulletin 14 (Sept. 2003). Parametric studies were then performed until good agreement was obtained with the field load/deflection response of the piles. The final soil parameters were in good agreement with the prior parameters, but not exact, because there were variations in the subsoil stratigraphy and the stress path was different for the horizontally loaded piles than the vertically loaded underreamed piers. The soil parameters used in the final FE analysis are summarized in Fig. 6.
- The initial cycle of loading at small loads was not modeled due to the small elastic deflections that were measured.
- The second cycle of loading was modeled to check the hysteresis cycles. However, only 2 load/unload cycles were computed due to the fact that the load/deflection curves were almost linearly elastic.
- After the cycling, the pile was loaded to the last measured field load.

Subsoil	c' kPa (ksf)	ϕ' (deg)	Ψ (deg)	G^{ref}_o mPa (ksf)	E^{ref}_{50} mPa (ksf)	E^{ref}_{oed} mPa (ksf)	E^{ref}_{ur} mPa (ksf)	m	ν_{ur}	I_f
Stiff clay	19.1 (0.4)	20	1	48 (1000)	9.6 (200)	7.2 (150)	27.5 (575)	8	15	6
Stiff to very stiff clay	19.1 (0.4)	20	1	96 (2000)	12.0 (250)	9.6 (200)	34.5 (720)	8	15	6
Very stiff clayey sand	28.7 (0.6)	30	2	144 (3000)	16.8 (350)	14.4 (300)	69.0 (1440)	8	15	6
Very stiff clay	28.7 (0.6)	20	1	192 (4000)	14.4 (300)	12.0 (250)	41.4 (865)	8	15	6
Very stiff sandy clay	28.7 (0.6)	30	2	240 (5000)	16.8 (350)	14.4 (300)	47.9 (1000)	8	15	6

Fig 6: Optimized Soil Parameters

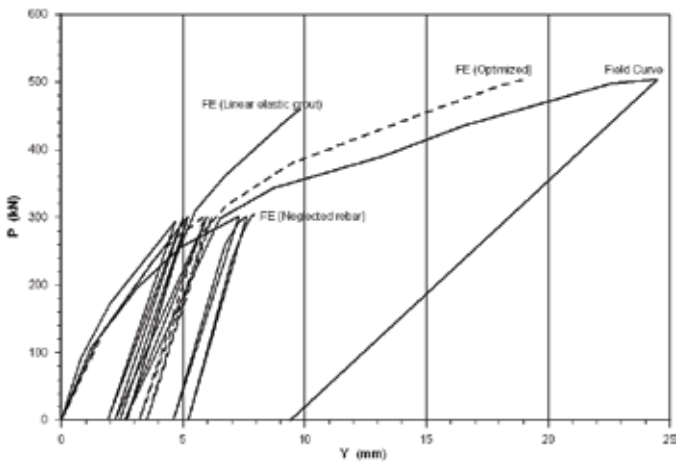

Fig 7: Comparison of Load/Deflection Curves for S Pile

Results

A graph of the field and FE computed load/deflection relationships for the S pile is shown in Fig. 7. The N pile was omitted for clarity because both the curves for the field loading and FE simulation plotted on top of each other. The FE computed load/deflection response of the pile without the shell is shown for comparison purposes. Also, the load/deflection response computed assuming linear-elastic parameters for the grout are shown.

A graph of the field and FE computed load/deflection curve for the E pile is shown in Fig. 8. As previously discussed, the W pile appeared to be an anomaly and is not shown. There were either subsoil variations in front of this pile, or there was an undetected defect in the pile.

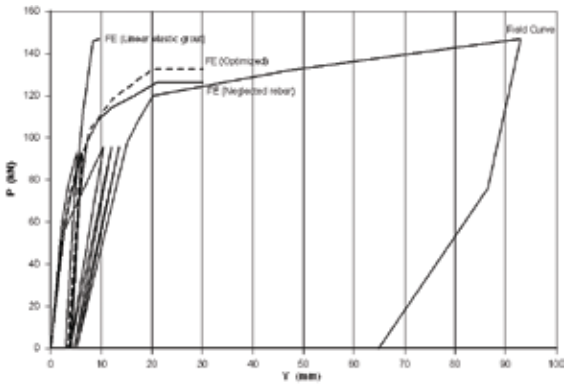

Fig 8: Comparison of Load/Deflection Curves for E Pile

A graph of the field measured and FE computed horizontal displacements with depth for the S & E piles is shown in Fig. 9. Note that FE predicts that a plastic hinge formed at about the same depth as measured in the field loading tests.

The initial FE computed load/deflection response of the piles using the optimized parameters is in excellent agreement with the loading tests. However, FE under predicts the deflections at the high loads.

The authors speculate that the piles as modeled in the FE analysis are stiffer than the field piles. The tension stress of the grout had been input so that the grout would crack and reduce the moment of inertia of the pile during the FE loading phases. However, the fact that the steel shell modeled in the FE analysis is located at the perimeter of the piles probably restricted the tension cracks that would be expected form between the rebar and outer edge of the field piles. Also, PLAXIS has published a notice that the interface elements for round piles have corners in the FE geometry that makes the interface behavior stiffer than would occur under field conditions (see Plaxis website).

The FE computed load/deflection response of the ACIP piles without the steel shell was somewhat softer than for the field piles. This occurs because of the reduced moment of inertia resulting from neglecting the rebar, and the fact that more deflections occur during loading increasing the tensile strains.

The FE computed load/deflection response of the ACIP piles assuming linear elastic properties for the grout was considerably stiffer than for the field piles. This occurs because the effective moment of inertia was not being reduced when the mobilized tensile stresses exceeded the tension cut off stress. These observations highlight the advantages of using a proper constitutive model for the grout so that the effective moment of inertia is automatically reduced during FE loading.

The good correlations are due to parameter studies, not simply selecting the correct input data for the initial computation. FE cannot be expected to model the load/deflection response within ±25 percent on a common basis because the stress/strain behavior of soil is very complex, and the uncertainty of selecting appropriate strength/deformation properties of the soil when there is considerable data scatter. Also, the strength/deformation properties of the pile materials must be properly accessed. It is possible that there might be other combinations of soil and pile properties that could result in correlations as well as those determined in this study.

Conclusions

The FE computed load/deflection response of the ACIP piles bearing in stiff to very stiff clay correlated well with results of the full scale lateral load tests. The small strain hardening soil model in PLAXIS 3D Foundations can be used in predicting the lateral load/deflection response of piles. However, additional research needs to be performed to better model ACIP piles with internal reinforcing steel if deflections are large enough to cause tension cracks in the grout.

References:

- K.M. Hassan, M.W. O'Neill, and C. Vipulanandan, Specifications and Design Criteria for the Construction of Continuous Flight Auger Piles in the Houston Area, FHA report UH 3921-1, 1998.

- L.J. Mahar and M.W. O'Neill, Geotechnical Characterization of Desiccated Clay, Journal of Geotechnical Engineering, ASCE, January, 1983, pp. 56-71.

- M.W. O'Neill, National Geotechnical Experimentation Site – University of Houston, Geotechnical Special Publication No. 93, 2000, pp. 72-101.

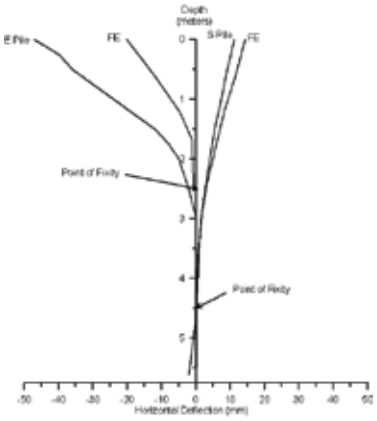

Fig 9: Delecftions with Depth